Full paper

Validation of UAV Wing Structural Model for Finite Element Analysis

Gunasegaran Kanesan*, Shuhaimi Mansor, Ainullotfi Abdul-Latif
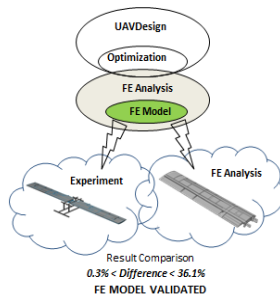
Aeronautics Laboratory, Faculty of Mechanical Engineering, Universiti Teknologi Malaysia, 81310 UTM Johor Bahru, Johor Malaysia

Corresponding author: gunasegaran2@live.utm.my/ guna8825@gmail.com

Article history

Graphical abstract

Abstract

Finite element method is increasingly used in the analysis of aircraft structures, including Unmanned Aerial Vehicles (UAVs). The structural model used for finite element analysis however needs to be validated in order to ensure that it correctly represents the physical behaviour of the actual structure. In this work, a case study of a straight, unswept and untapered wing structure made of composite material subjected to aerodynamic loading was modelled and analysed using finite element method. Four-noded, reduced integration shell elements were used, with structural components attached by adhesive joints modelled using tied surface constraints. For the validation process an experimental set-up of the actual wing was loaded using sandbags to simulate the aerodynamic loads. The deflection of the wing at three key locations were obtained and compared between both methods. It was found that the difference between both results ranges between 0.3% (at the tip) to 36.1% (near the root, for small deflections).

Keywords: Finite elements; unmanned aerial vehicles; wing structural analysis

■1.0 INTRODUCTION

An unmanned aerial vehicle (UAV) is a pilotless aircraft controlled by a ground unit from a control room. The interest in UAV development is growing in recent years due to the possibilities of utilizing relatively non-expensive airplanes without the human presence on board when the mission involves long operational time and severe risks [1]. In modern airplane designs, composite materials are integral part of the structures. The advancement in structures and materials especially the introduction of composite materials used for UAV construction is one of the great factor contributing to continuous development in UAV industry [2]. However, the design is not optimised in terms of weight due to the lack of accurate data, or even the use of appropriate composite is abandoned in favour of the more familiar metals [3].

A research to develop a methodology to design and optimise the UAV wing structure is conducted and part of the research is validating the finite element model of the wing used for analysis. This validation work is presented in this paper. Validation is a process by which the predictive capabilities of a model are tested with experimental data [4]. The model for FE analysis in this research was generated by using ABAQUS/CAE (version 6.11), FE analysis commercial software. The model was subjected to implicit FE analysis.

Several papers have been published regarding the finite element modelling of the airplane wing. Mazhar and Khan [5] presented the structural design methodology for the wing of an UAV. In their paper, finite element method used for strength and stiffness analysis of the wing is presented. Gadomski *et al*. [6] presented detailed structural design and optimization for two medium altitude long endurance UAV's and the corresponding FE analysis. Ostergaard *et al*. [7] presented the FE analysis used for Airbus A380 certification. In their research, the FE analysis for the certification process was conducted by using ABAQUS/CAE. Some important information regarding the assumptions made for FE analysis were also presented. Nurhaniza *et al*.[8] presented the method for FE analysis of composite material used for aerospace application. A simple method to simulate tensile testing was presented in their paper.

The basic principle of FEM is discretisation of the continuous structure into substructures. The original structure was assumed to have infinite numbers of degree of freedom. On the other hand, the substructures are assumed to have finite numbers of degree of freedom. The substructures obtained from discretisation process are called as finite elements. This discretisation is defined by the finite element mesh made up by elements and nodes [9].

These elements are considered to be interconnected at nodes [10]. In mechanical point of view, nodes are the coupling points of elements where the displacements of the coupled elements are compatible. Meanwhile in mathematical point of view, nodes are seen as basic points for the approximate functions of displacements for a finite element and at these nodes the

displacements are compatible. It must be noted that in this research all considerations are restricted to the displacement method [9].

Ostergaard *et al.* stated that the way the structure is modelled and how the interactions between the structural parts are represented will define the effectiveness and accuracy of the analysis output [7].

■2.0 MODELLING OF THE UAV WING

The UAV wing used in this analysis consists of two spars, 10 leading edge ribs, 10 centre ribs, two outboard ribs, five trailing edge ribs and three parts of skins as major structural components. Some of the important parameters of the wing are shown in Table 1. The detailed drawing of the wing is shown in Figure 1.

Table 1 Important parameters for UAV wing

Parameter	Value
Span length (b), m	5.1257
Chord length (c), m	0.5886
Weight, kg	45.4
Number of spars	2
Number of ribs	12

The major structural components of the wing were made of composite materials except for fasteners, brackets which attach the wing to the fuselage, and some other minor components. Carbon fibre fabric, unidirectional carbon fibre, kevlar, glass fibre and aramid honeycomb core were used in the construction of these components, with epoxy resin as the matrix. The wing major structural components with their corresponding composite layers are given in Table 2.
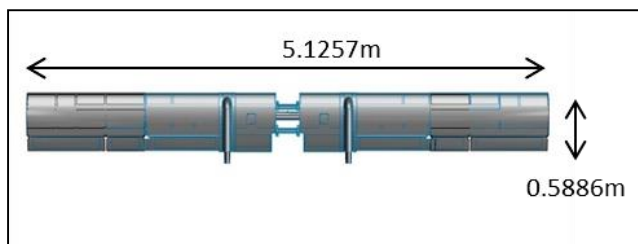

Figure 1 UAV complete wing plan view

The geometrical modelling of the wing structural components was conducted in Solidworks and imported into Abaqus/CAE. Since the UAV wing was assumed to be symmetrical, only half of the wing was modelled to reduce the total number of elements used in analysis and hence reduce the computational time. The mechanical properties of the materials used are given in Table 3. Figure 2 shows the assembled components of the UAV wing before the generation of mesh.

The generation of mesh is important in FE analysis since the nodes generated define the output criteria of the analysis. According to Reddy [11], the following considerations need to be addressed before generating the mesh:

- The mesh should accurately represent the geometry of the computational domain and loads.
- The mesh should be that the large gradients (displacements or stresses) in the solution are adequately represented.
- The mesh should not contain elements with very large aspect ratio.

Table 2 Composite laminates for wing structural component

Elements	Total No. of Layers	Material
NACA 4415 Wing Skin	5	Carbon Fibre Fabric, Kevlar Veil, Honeycomb Cores
Main Spar	8 to 12	Carbon Fibre Fabric ±45º and 0/90, Carbon Uni-tape
Outboard Main Spar	8 to 12	Carbon Fibre Fabric ±45º and 0/90, Carbon Uni-tape
Aft Spar	6 to 10	Carbon Fibre Fabric ±45º and 0/90, Carbon Uni-tape
Outboard Aft Spar	4 to 8	Carbon Fibre Fabric ±45º and 0/90
Leading Edge Rib	5	Carbon Fibre Fabric ±45º , Kevlar Veil
Centre Edge Rib	5	Carbon Fibre Fabric ±45º , Kevlar Veil
Trailing Edge Rib	5	Carbon Fibre Fabric ±45º , Kevlar Veil
Hinge Rib	5	Carbon Fibre Fabric ±45º and 0/90
Outboard Rib	5	Carbon Fibre 0/90 , Kevlar Veil

*angle taken with reference of global X-axis

Table 3 Elastic properties of the material used in modelling [12-15]

Material	E_{11} (GPa)	E_{22} (GPa)	v_{12}	G_{12} (GPa)
Carbon Fibre Fabric/Epoxy	70	70	0.1	5
CarbonUnitape /Epoxy	140	10	0.3	5
Kevlar/Epoxy	78.5	5.52	0.34	2.07
Honeycomb	0.1287	0.0126	0.2606	0.0016
Glass Fibre/Epoxy	38.36	38.36	0.156	6.4

Given the large scale of the model and the nature of the structures, shell elements were used to represent all components, except for the brackets, for which solid elements were used. This was in line with what was stated by Ostergaard *et al.* [7] who recommended S4 and S4R four-noded shell elements in ABAQUS for most analysis of aircraft structures, given their efficient and robust nature. Laulusa *et al.*[16] also stated that the S4R element is effective in modelling shell structures because it can reduce lots of computational time and cost. S4R elements are similar to S4 elements except that they have reduced number of integration points [17]. In this analysis, S4R type elements were used in most parts except for some critical areas such as sharp edges or corners. A total of 243,337 elements were generated for the analysis. The meshing was refined at the spar-fuselage attachment regions, as these areas were expected to be the most critical areas in the model, with higher likelihood of failure to occur there first. The number of elements generated for each parts are shown in Table 4.
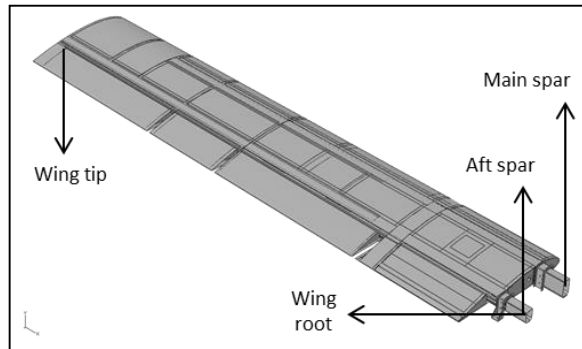
Figure 2 UAV wing geometry drawing

Table 4 The number of elements of wing major components

Elements	Number of elements
Main Spar	68399
Aft Spar	62089
Main Wing Top Skin	6411
Inboard Top Skin	10330
Inboard Lower Skin	16484
Outboard Lower Skin	8575
Leading Edge Rib	555
Center Edge Rib	687
Trailing Edge Rib	342
Outboard Rib	853

The interactions between the structural components are important in determining the effectiveness of model as stated by Ostergaard *et al.* [7]. Adhesive joints were used to attach major structural components in the actual wing structure. For this analysis, these adhesive joints were considered as tied surface constraints with zero thickness between the tied surfaces. This was adequate for most of the detailed analyses, since the elastic stiffness of a thin adhesive layer was unlikely to be a key variable in overall structural response [7]. Apart from adhesives, some of the structural components were attached by using extra carbon fibre layers. The epoxy resin used to attach these components with the extra layer was also modelled as tied surface constraint.

The values of force or displacement degrees of freedom at some nodal points of the model were specified in some cases. These known conditions were assigned in FE analysis as boundary condition in the model [18]. In this analysis, there were two important boundary conditions which needed to be specified. The first was the attachment of the C-shaped bracket to the fuselage. Since the fuselage was not included in the model, the bottom surface of bracket was defined as fixed. This indicated that all the displacements and rotations at the bottom surfaces of the brackets were set to zero i.e. $U1=U2=U3=UR1=UR2=UR3=0$ [17]. The second set of boundary conditions defines the symmetrical condition of the wing. In this analysis, the spars of the wing were set to be symmetrical about the XY-plane, $U1=UR2=UR3=0$ [17]. The applied boundary conditions are circled in Figure 3 and Figure 4.

The loads were applied on the model as distributed pressures on the wing skin. These pressures were derived from the loads used in experimental procedures, simulating aerodynamic loads. The information on these loads is given in the following section.
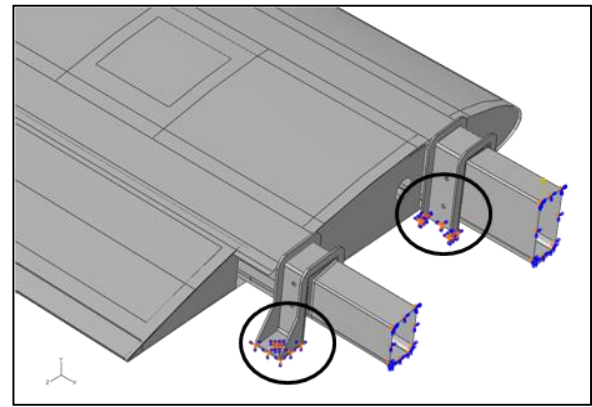

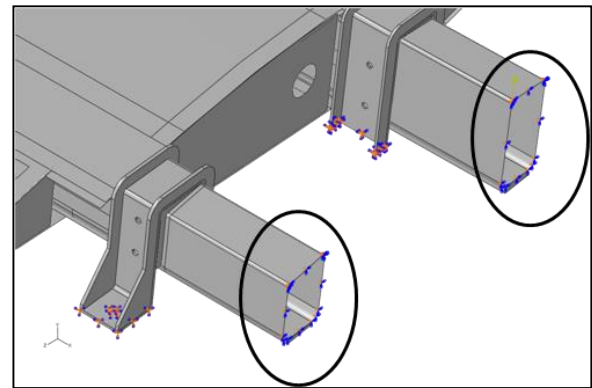**Figure 3** Boundary conditions where the bottom of the brackets were fixed

Figure 4 Boundary conditions where the spars were set to be symmetrical about the XY-plane

■3.0 EXPERIMENTAL PROCEDURES

The experiment was conducted on the UAV full wing provided by Unmanned System Technology Sdn Bhd. Sandbags weighing 1 kg each were used to represent the aerodynamic loads on the wing. The wing was attached to a stationary rig using C-shaped brackets. The brackets were fixed at the root of the spars and screwed into the rig. Figure 5 and Figure 6 show how the wing was fixed to the rig. The circled objects in Figure 6 indicate the attachments of the brackets to the test rig. The wing was positioned upside down since gravitational loads (downwards) were used to simulate upwards lift in flying condition.

Tests were conducted to obtain the deflections of the wing under bending mode. Various loading values were used during the experiments. Dial gauges were used to obtain the deflections at three different locations: 250 mm, 350 mm and 2560 mm (tip) from the centreline of wing. Bending tests on the wing were conducted with nine different loading values. The loads were applied on the bottom skin of the wing directly on top of main spar and aft spar. The bottom skin was divided into six sections and each section carried different loadings in the form of sandbags. The area for the each loading section was $0.01524m^2$. The loadings were applied in uniform and elliptical conditions spanwise. Table 5 shows the loading cases (1-9) applied on wing throughout the experiment.

Figure 5 Wing-to-rig attachment

Figure 6 Bracket-to-rig attachment

■4.0 RESULTS AND DISCUSSION

The loadings shown in Table 5 were transformed into corresponding pressure values. Pressures were found by dividing the area to loads in respective sections. The nodes at the exact locations of dial gauges were identified. Deflection output values were recalled for these nodes after each analysis.

The results for both experiments and FE analyses are shown in three different tables. Each table shows the results for each dial-gauge location and their respective differences.

The differences between deflection values for bending tests and FE analyses are small for the tip of wing compared to the deflections at the other two locations. It was found that the difference between both results ranges between 0.35% (350 mm from centreline) to 36.1% (near the root). The differences between both results at locations 350 mm and 2560 mm (tip) range between 0.35% to 16.4%.

The differences obtained for location 250 mm (near root) is higher due to the smaller deflections obtained at that location. A small difference in the values could result in larger percentage difference between the values. Hence, the results from this location were excluded from the validation process.

Nurhaniza et al. [8] stated that the percentage of error between the results from Abaqus and experiments has a range of 10-25%. Their study was conducted on the composite wing of an aircraft wing. Autio et al. [19] stated that usually the error results given by commercial FEM programs compared to measured results should be less than 20%. By comparing the deflections results at locations 350 mm and 2560 mm (tip), the registered percentage of differences are less than 16%. This is adequate to validate the UAV wing finite element model.

Table 5 Loading conditions used in wing bending test

No	Total Load (kg)	Spar	0-30	30-60	60-90	90-120	120-150	150-180
			Weight (kg)					
1	32	MS	10	10	7	5	-	-
		AS	-	-	-	-	-	-
2	39	MS	10	10	7	6	4	-
		AS	-	-	-	-	-	-
3	39	MS	7	7	5	4	3	1
		AS	3	3	2	2	1	1
4	40	MS	8	7	5	4	3	1
		AS	3	3	2	2	1	1
5	41	MS	8	7	6	4	3	1
		AS	3	3	2	2	1	1
6	42	MS	8	7	6	5	3	1
		AS	3	3	2	2	1	1
7	43	MS	8	7	6	6	3	1
		AS	3	3	2	2	1	1
8	44	MS	8	7	6	6	3	1
		AS	4	3	2	2	1	1
9	45	MS	8	8	6	6	3	1
		AS	4	3	2	2	1	1

The header spans: "Distance from the start of lower skin (cm)" over columns 0-30, 30-60, 60-90, 90-120, 120-150, 150-180; "Weight (kg)" spans all distance columns.

Table 6 Results for deflection at 250 mm from wing centreline

No	Deflection at 250mm (mm)		Difference (%)
	Bending Test	**FE Analysis**	
1	0.460	0.527	12.71
2	0.824	0.702	17.38
3	0.830	0.654	26.91
4	0.835	0.661	26.32
5	0.852	0.676	36.05
6	0.879	0.696	26.29
7	0.859	0.716	19.97
8	0.909	0.721	26.16
9	0.955	0.732	30.46

Table 7 Results for deflection at 350 mm from wing centreline

No	Deflection at 350 mm (mm)		Difference (%)
	Bending Test	**FE Analysis**	
1	0.880	1.053	16.43
2	1.410	1.415	0.35
3	1.420	1.328	6.93
4	1.430	1.340	6.72
5	1.450	1.372	5.72
6	1.480	1.413	4.76
7	1.560	1.454	7.29
8	1.630	1.463	11.42
9	1.720	1.485	15.83

Table 8 Results for deflection at 2560 mm from wing centreline

No	Deflection at 2560 mm (mm)		Difference (%)
	Bending Test	FE Analysis	
1	8.660	8.904	2.74
2	12.320	12.845	4.09
3	12.720	12.599	0.96
4	13.530	12.666	6.82
5	13.860	12.930	7.17
6	14.140	13.330	6.07
7	14.840	13.727	8.11
8	15.220	13.799	10.30
9	15.820	13.953	13.38

■5.0 CONCLUSION

In this study, the finite element model used for FE analysis has been validated. Comparing the results from the experimental tests and the FE analysis using ABAQUS/CAE, it was found that the difference between both results ranges between 0.35% to 16.4%.

However, the method used for the validation still has room for improvements, including:

(1) The meshing of the model need to be more refined. The number of elements was set to 243,337 due to the limited computational capabilities.
(2) The deflection should be measured at more locations during the experiment to increase the reliability of results.
(3) Digital dial gauges should be used instead of analogue dial gauges at the locations near to fixed bracket areas. This is to increase the precision for the deflection values obtained since the deflection values at this area are too small.

Acknowledgement

References

[1]   A.F. Accardo, F. Ricci, P. Basso. 2000. Design and Development of Low Altitude Unmanned Aerial Vehicle. *22nd International Congress of Aeronautical Science ICAS*. Harrogate UK.
[2]   P. Yong-Bin, N. Khanh-Hung, K. Jin-Hwe, C. Jin-Ho. 2011. Structural Analysis of a Composite Target-drone. *International Journal of Aeronautical & Space Science*. 12:84–91.
[3]   O.I. Okoli, A. Abdul-Latif. 2002. Failure in composite laminates: Overview of an attempt at prediction. *Composites Part A: Applied Science and Manufacturing*. 33(3):315–321.
[4]   B. Szabó, I. Babuška. 2011. *Introduction to Finite Element Analysis: Formulation, Verification and Validation*. West Sussex: Wiley.
[5]   F. Mazhar, A. M. Khan. 2010. Structural Design of a UAV Wing Using Finite Element Method. *51st AIAA/ASME/ASCE/AHS/ASC Structures, Structural Dynamics, and Materials Conference*. American Institute of Aeronautics and Astronautics
[6]   J. Gadomski, B. Hernik, Z. Goraj. 2006. Analysis and optimisation of a MALE UAV loaded structure. *Aircraft Engineering & Aerospace Technology: An International Journal*. 78(2):120–131.
[7]   M.G. Ostergaard, A.R. Ibbotson, O.L. Roux, A.M. Prior. 2010. Virtual testing of aircraft structures. *CEAS Aeronaut Journal*. 1:21.
[8]   M. Nurhaniza, M.K.A. Arifin, A. Ali, F. Mustapha, A.W. Noraini. 2009. Finite element analysis of composites materials for aerospace applications. *9th National Symposium on Polymeric Materials, Materials Science and Engineering*.
[9]   H. Altenbach, J. W. Altenbach, W. Kissing, 2004. *Mechanics Of Composite Structural Elements*. New York: Springer.
[10] A.A. Becker, R.C. Baker. 2004. *An Introductory Guide to Finite Element Analysis*. London: Professional Engineering.
[11] J.N Reddy, 1993. *An Introduction to The Finite Element Method*, New York: McGraw-Hill.
[12] M.H. Datoo. 1991. *Mechanics of Fibrous Composites*. United Kingdom: Elsevier Science.
[13] D. De Renzo. 1988. *Advanced Composite Materials: Products and Manufactures*. New Jersey: Noyes Publications.
[14] O.I. Okoli. 1997. *Experimental Determination of Transient Dynamic Response of Fibre Reinforced Polymer Composites*. PhD thesis, University of Warwick, UK.
[15] T. Bitzer. 1997. *Honeycomb Technology: Materials, Design, Manufacturing, Applications And Testing*. Springer.
[16] A. Laulusa, O. Bauchau, J.Y. Choi, V.B.C. Tan, L. Li, 2006. Evaluation of some shear deformable shell elements, *International Journal of Solids and Structures*, 43(17): 5033-5054
[17] Abaqus Version 6.9EF-1. 2009. Abaqus Documentation, Dassault Systems, Providence, RI, USA
[18] O.O. Ochoa, J.N. Reddy. 1992. *Finite Element Analysis Of Composite Laminates*. Dordrecht: Kluwer Academic.
[19] M. Autio, H. Parviainen, A. Pramila. 1992. Accuracy of the finite element method in analyzing laminated plate and pipe structures. *Mechanics of Composite Materials*. 28(3):236–245.